

Article

Optimization Using Response Surface Methodology (RSM) for Biodiesel Synthesis Catalyzed by Radiation-Induced Kenaf Catalyst in Packed-Bed Reactor

Nur Haryani Zabaruddin ^{1,2} , Luqman Chuah Abdullah ^{1,3,*} , Nor Hasimah Mohamed ^{2,*} 
and Thomas Shean Yaw Choong ³

¹ Institute of Tropical Forestry and Forest Products, Faculty of Engineering, Universiti Putra Malaysia, Seri Kembangan 43400, Malaysia; nurharyanizaba@gmail.com

² Radiation Processing Division, Malaysian Nuclear Agency, Kajang 43000, Malaysia

³ Department of Chemical and Environmental Engineering, Faculty of Engineering, Universiti Putra Malaysia, Seri Kembangan 43400, Malaysia; csthomas@upm.edu.my

* Correspondence: chuah@upm.edu.my (L.C.A.); shima@nuclearmalaysia.gov.my (N.H.M.);
Tel.: +603-9769-6288 (L.C.A.)

Received: 17 August 2020; Accepted: 21 September 2020; Published: 14 October 2020



Abstract: In this study, continuous transesterification of refined palm oil by using radiation-induced kenaf denoted as anion exchange kenaf catalyst in a packed-bed reactor was developed. The application of full factorial design and response surface methodology (RSM) based on the central composite design (CCD) was used to design the process and analyzed the effect of reactor operating variables such as packed bed height, the molar ratio of oil to ethanol and volumetric flow rate on the production of fatty acid ethyl ester (FAEE). The statistical analysis results showed that all three operating parameters affect the reaction efficiency significantly. The optimum conditions were determined to be 9.81 cm packed bed height, a molar ratio at 1:50, and a volumetric flow rate of 0.38 mL min⁻¹. Three tests were carried out to verify the optimum combination of process parameters. The predicted and actual values of molar conversion fatty acid ethyl ester (FAEE) molar conversion were 97.29% and 96.87%, respectively. The reusability of kenaf fiber-based catalysts is discussed with a specially highlighted on fiber dissolution, leaching, and fouling. Nevertheless, the impurities absorption properties of anion exchange kenaf catalyst towards biodiesel production could eventually simplify the biodiesel purification steps and cost. In sum, anion exchange kenaf catalyst shows the potential commercial applications to transesterification of FAEE in a packed-bed reactor.

Keywords: biodiesel; fatty acid ethyl esters; transesterification; heterogeneous catalyst; natural fiber; packed bed reactor; response surface methodology; central composite design

1. Introduction

The consciousness of environmental problems and energy issues related to fossil fuels has encouraged many researchers to explore the possibility of using renewable fuels instead of fossil fuels. Biodiesel seems remarkably interesting to be investigated for some advantages focusing on its renewability, economic aspects, and environmental impacts. The most interesting criteria are biodiesel shows a comparable physicochemical characteristic and ignition performance compared with petroleum diesel [1–5].

Biodiesel is simply defined as a liquid fuel derived from vegetable oil, animal oil, and fats, and waste cooking oil by using various approaches and the most common biodiesel technologies

employ homogenous base catalysts such as potassium hydroxide, sodium methoxide, and sodium hydroxide (NaOH) to accelerate the transesterification process in a batch system. The batch homogenous catalytic is a simple, cheap and short time, however, the major drawbacks associated with the process are that the homogeneous catalyst is corrosive, difficult to reuse, and unnecessarily complex separation of by-product [5]. Although this conventional catalyst achieves great conversion yields; it is not suitable to be used to produce biodiesel from high free fatty acid feedstocks as it is highly sensitive to the presence of water and free fatty acid (FFA) which leads to soap formation and hindered the conversion of biodiesel. The additional complicated and costly purification processes for homogenous catalyzed batch transesterification can cause an undesirable effect on the economic and environmental [6].

Heterogeneous catalysts are widely used for biodiesel production due to the low cost, thermal stability, easy recovery, and regeneration. In comparison to the homogeneous catalyst, heterogeneous catalysts are known as a solid catalyst that has the ability to catalyze esterification and transesterification both to low and high FFA oils due to the high concentration of an acid or basic active sites [7]. Besides, it also has high water tolerance properties, easy product separation and possible to reuse for further reactions. Most of the heterogeneous catalysts used especially solid alkaline catalysts have provided high yields [8–10]. Anion exchange resins are one of the example solid alkaline catalysts that are made of divinyl-benzene copolymers, styrene, and quaternary ammonium functional. The main feature of ion exchange resin is the ability of their functional groups to dissociate in liquid media and exchange ions as well as possess a chemisorption property. An experimental study by [11] has revealed that the activity of commercial anion exchange resin was said to be reasonably comparable to those of the homogeneous base catalysts. Interestingly, it also stated that anion exchange resin used not only act as a catalyst but as an absorbent as well. Anion exchanger adsorbed impurities of the feedstock, free fatty acid, water, glycerol, and dark brown pigment that is saturated on the resin. The catalytic ability of the resin was restored through the washing and regeneration process. Ueki et al. [12] are claimed to be the first application of anion exchange fiber for biodiesel fuel production. The catalyst was developed using radiation-induced graft polymerization of 4-chloromethyl styrene onto a synthetic nonwoven polyethylene (NWPE) fabric and functionalized with trimethylamine (TMA) and further treatment with NaOH. They reported that the anionic exchange fiber performance was three times faster than that of commercial anion exchange resin, Diaion PA306s. This excellent performance is believed due to the small diameter of fiber that has ten times smaller as compared to the sphere-shaped resin. According to [13], the diameter granular ion exchanger and fibrous ion exchanger is 0.5 mm and 22 μm , respectively. The surface of the ion exchange fiber can be as high as 2000–4000 m^2/g . Thus, fiber has a potentially much higher supporting capacity for active sites than resins.

Synthetic anion exchange resin and fiber, however, produce from non-renewable and non-biodegradable organic materials. Additional problems faced by solid catalysts are microporosity, leaching, toxic and expensive [14,15]. A green solid catalyst also known as a bio-based catalyst is a term referring to a type of catalyst derived from natural sources such as plant fiber and biomass. The exploration of greener materials as an alternative from conventional solid catalysts for biodiesel production has been reported by numerous studies such as natural fiber, volcanic rock, waste shell, animal bones, waste eggshell and, activated carbon-supported catalyst [16–21]. Natural fibers have the advantage of environmentally friendly, lightweight, abundant, and low cost compared to synthetic material. Lignocelluloses such as rice hull, sugarcane bagasse, and wheat straw are successfully converted into weak base anion exchanger to treat water contaminated with nitrate [22]. The natural fiber is considered as designer fibers since their properties can be appropriately modified and established for different purposes. Although references [23–25] have been found for the synthesis of anion exchanger based on natural fiber, the specialty of this research lies in the modification of kenaf fiber to anion exchanger by radiation-induced graft polymerization of 4-vinyl-benzylchloride followed by amination with trimethylamine. Kenaf fiber (species *Hibiscus cannabinus* L.) is easily found in abundance in Malaysia and relatively low capital investment which great to be explored as a new

utilization as a trunk polymer for grafting co-polymerization to produce catalyst that can be used in production of biodiesel.

In a laboratory-scale experiment, transesterification of heterogeneous processes could be run in a continuous mode with a packed-bed continuous flow reactor, unlike homogeneous catalysts which are suitable for batch production only. The continuous-flow reactors are preferred over batch processes, especially in large-capacity commercial production because of the major drawbacks of a batch catalytic process such as low productivity due to the time consuming for the batch-to-batch process, inconsistency in product quality as each batch is unique and required more intensive labor and energy as compared to continuous operation. The advantages of biodiesel produced using continuous operation are more constant in quality [26].

Another technical issue associated with the batch homogeneous catalytic process is poor mixing performance. This problem can be overcome as suggested [27] in the application of a packed-bed reactor (PBR) for the transesterification process as it facilitates effective mixing of two-phase liquid-liquid reaction due to the formation of stable emulsion from the immiscible oils-alcohol mixture. In the case of heterogeneous catalysts, increased mass transfer limitations occur as the reaction is transformed from biphasic liquid-liquid reaction to three-phase solid-liquid-liquid reactions. Thus, PBR will improve mass transfer and accelerate the rate of biodiesel production reactions. Since heterogeneous catalysts were easily packed in the reactor and simply separated from the products. Furthermore, the water-washing process and neutralization steps were avoided [11,28]. In results, water containing impurities from this process was greatly reduced, and the biodiesel treatment cost was also minimized [29].

This study aims to utilize a bio-based heterogeneous catalyst derived from kenaf fiber fabricated by radiation-induced graft polymerization for transesterification of refined palm oil into biodiesel in a packed-bed reactor. A fiber-based anion exchange catalyst can be considered as a good substitute for its potential to help in reducing the shortcoming and risks associated with the usage of homogeneous catalysts. Moreover, anion exchange kenaf has numerous environmentally friendly advantages compared to a synthetic catalyst. Therefore, the up-flow configuration experimental setup was developed and studies for the analysis of the operating parameters and its effect using the design of the experiment (DOE) will enhance in-depth knowledge of the continuous transesterification process packed with anion exchange kenaf catalyst.

2. Materials and Methods

2.1. Materials

The refined palm oil (Buruh, Malaysia) was purchased from the local market. The developed radiation-induced kenaf catalyst was fabricated by radiation-induced graft polymerization method using electron beam irradiation at a dose of 150 kGy. Additional detailed description of the catalyst fabrication methods can be found in a previous study by [30]. The standards of rac-glycerol 1-monooleate (MAG), ethyl oleate (FAEE), 1,3-dioleate (DAG), glyceryl trioleate (TAG), and commercial strong base Amberlite® IRA402 resin in chloride form were purchased from Sigma Aldrich (St. Louis, MO, USA). All solvents were high-performance liquid chromatography (HPLC) grade. Acetonitrile, n-hexane, 2-propanol, and ethanol were obtained from Merck KGaA (Darmstadt, Germany).

2.2. Reactor Setup

The continuous transesterification was conducted using a bench-scale bed reactor packed with the fabricated catalyst. The equipment was successfully assembled and commissioned before proceeding with the preliminary experiments.

Figure 1 shows a schematic diagram of a continuous transesterification system in the concurrent up-flow configuration. The catalyst was packed inside a simple glass column (Ace Glass Inc., New Jersey, USA) with an inner diameter of 0.7 cm and a height of 15 cm. The reactor and peristaltic pump line were initially test run using the water to detect any leakage followed by the test of the chosen

parameters required to carry out a continuous transesterification of palm oil and ethanol in the present of kenaf catalyst. The bed porosity, ϵ_b is the fraction of the volume of space between the solid particles of the catalyst to the total empty reactor volume and it is defined using the following Equation (1).

$$\text{Bed porosity } (\epsilon_b) = 1 - \frac{w_c / \rho_c}{\pi h (d/2)^2} \quad (1)$$

where w_c is the weight of the catalyst and ρ_c the density of wet kenaf catalyst in ethanol. The continuous transesterification performance was observed for various residence times. Residence times in the reactor which are corresponding to volumetric flow rates. Catalytic packed bed height can be directly correlated with the catalyst weight into the column reactor by following Equation (2).

$$h = 2.85462 \times w_c \quad (2)$$

where h is the bed height in centimeters and w_c is the catalyst weight in grams.

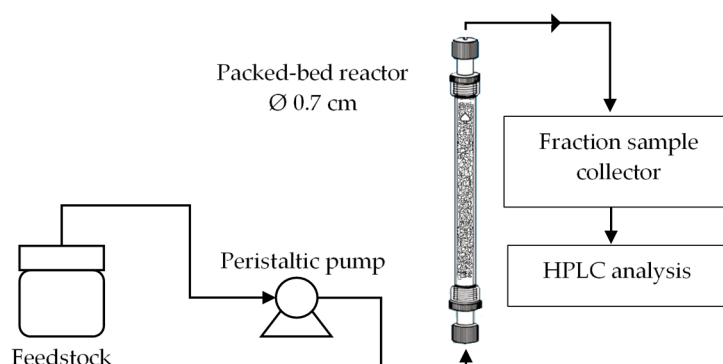


Figure 1. Schematic diagram of a continuous transesterification system.

2.3. Catalyst Preparation and Characterization

The catalyst was prepared using a radiation-induced graft polymerization technique. Kenaf fiber was weighed and neatly stacked in $15 \times 10 \text{ cm}^2$ polyethylene zipper bag and it was purged with nitrogen gas to remove any oxygen contained in the bag. Kenaf fibers were irradiated in the inert condition under an electron beam a dose of 150 kGy. After irradiation, kenaf fiber was added into glass ampoule. The air in the glass ampoule was evacuated by connected to a vacuum line for 10 minutes before immersing in an emulsion containing composed of 5 wt%, 4-vinyl-benzylchloride (VBC), 0.5 wt% Tween 20 and 94.5 wt% deionized water as to avoid radical deactivation during radiation-induced graft polymerization for 24 h under room temperature. The VBC-grafted kenaf fibers were functionalized by immersed 8 h in trimethylamine (TMA) solution.

Moreover, the characteristics of the prepared induced VBC-grafted kenaf catalyst were determined. The field emission scanning electron microscope (FESEM) analysis by Carl Zeiss GeminiSEM 500 equipped with energy-dispersive x-ray spectrometry (FESEM-EDX) was carried out room temperature and used accelerating voltages of 0.02–30 kV to study the surface morphology of the induced VBC-grafted kenaf catalyst. The samples were first sputter-coated with a thin layer of platinum and then observed at a magnification of 150 kX, and 1500 kX. The TMA group density for the catalyst was measured by analysis of their nitrogen using carbon, hydrogen, nitrogen and sulphur analyzer (CHNS); CHN628s by Leco, UK. The conventional titration method was carried out to determine the ion exchange capacity of the induced VBC-grafted kenaf catalyst. About 1 g catalyst was placed in a conical flask with a stopper containing exactly 200 mL of 0.1 N HCl solution. Then, 10 g of NaCl was added and the flasks were left shaken in a shaker for 4 h at room temperature. Next, the solution was filtered, and 50 mL aliquots were subjected to back titration using 0.1 N volumetric standard NaOH using phenolphthalein indicator. Surface area, pore-volume, and average pore diameter performed by

using a Micromeritics ASAP 2020 surface analyzer. The catalyst samples (0.35–0.5 g) were degassed through a two-stage temperature ramping under a vacuum of < 10 mmHg, followed by sample analysis at 77 K using nitrogen gas.

2.4. Catalyst Screening

The performance of the fibrous catalyst was evaluated in batch-wise transesterification prior to continuous flow studies. Additionally, the catalytic performances compared between anion exchange kenaf catalyst and commercial Amberlite® IRA402 resin in chloride form. To produce the anionic type of ion exchanger, about 0.1 g (dry weight) of anion exchanger catalyst was immersed in 1 M Sodium hydroxide aqueous solution (NaOH) for 30 min to introduce the hydroxide (–OH) on the surface of the catalyst. Then, the anion exchanger catalyst was washed with deionized water after 30 min of NaOH treatment. The transesterification reaction was carried out by steadily shaking the anion exchanger catalyst into 10 g of ethanol–palm oil (50:1) solution using a water bath shaker (Daihan, model WSB-18) at room temperature up to 24 h. Then, the reaction mixture was analyzed using HPLC.

2.5. Transesterification in the Packed Bed Reactor

The reactor was packed with radiation-induced kenaf catalyst and the adjustment of catalytic bed height is directly dependent on the weight of the catalyst into the reactor. The mixture of refined palm oil and ethanol was fed into a packed-bed reactor packed with radiation-induced kenaf catalysts in the concurrent up-flow using a peristaltic pump at a known flow rate based on selected CCD levels (Table 1). The reaction temperature was kept at room temperature. The sample was collected using an automatic fractional collector after 4 h of reaction time. About 100 µL sample aliquots were taken from the reaction mixture and were diluted in 2-propanol-n-hexane. The concentration of rac-glycerol 1-monooleate, ethyl oleate, 1,3-dioleate, and glyceryl trioleate was calculated by HPLC analysis.

Table 1. Experimental range and levels of the independent variables are in central composite design (CCD) and response surface methodology (RSM) for biodiesel production from refined palm oil using radiation-induced kenaf catalysts using packed bed reactor.

Parameters	Coded Levels				
	−1.682 (−α)	−1	0	+1	1.682 (+α)
X ₁ : Packed bed height (cm)	1.272	4	8	12	14.727
X ₂ : Volumetric flow rate (mL min ^{−1})	0.232	0.3	0.4	0.5	0.568
X ₃ : Molar ratio	33.182	1:40	1:50	1:60	66.818

2.6. HPLC Analysis

The quantification of rac-glycerol 1-monooleate (MAG), ethyl oleate (FAEE), 1,3-dioleate (DAG), and glyceryl trioleate (TAG) content in palm oil-based biodiesel were performed by reserved phase high-performance liquid chromatography (RP-HPLC). The analysis instrument consisted of an online degasser (model DGU-20A5R, Shimadzu, Kyoto Japan), a pump (model LC-20AD, Shimadzu) with a quaternary gradient system, an autosampler (model SIL-20ACHT UPLC, Shimadzu) with a 5 µL sample reservoir, ultraviolet-visible photodiode array (UV-VIS PDA) detector (model SPD-M20, Shimadzu), a column oven (model CTO-10AS VP, Shimadzu), and a data processor (model LC solution software, Shimadzu). A Phenomenex Kinetix C18 UHPLC column (150 mm × 2.1 × 2.1 µm) is used for the separation. The chromatographic separations of biodiesel and triglyceride were performed by a ternary gradient elution using ultra-pure water (A), acetonitrile (B), and 2-propanol-n-hexane (5:4, v/v) (C), as mobile phase with flow rate 1.0 mL min^{−1} start with 100% acetonitrile at 20 min and change to 30% acetonitrile + 70% 2-propanol-n-hexane from 20 to 35 min. The column temperature and UV detector were set at a wavelength of 205 nm and 40 °C respectively.

The percentage of molar conversion palm oil to biodiesel was calculated as follows:

$$\text{Molar conversion FAEE } (C_{\text{FAEE}}) = \frac{A_{\text{CFAEE}}}{A_{\text{CFAEE}} + A_{\text{CMAG}} + 2A_{\text{CDAG}} + 3A_{\text{CTAG}}} \times 100\% \quad (3)$$

where C_{FAEE} is the molar conversion of FAEE in %, A_c is a corrected area obtained after integration of the individual component peak identified by comparing the calculated relative retention time that of the selected reference standard peaks in the chromatogram.

2.7. Experimental Design

Transesterification of refined palm oil with radiation-induced kenaf catalysts was developed and optimized by using the response surface method of 2^3 (three factors each at two levels) central composite design (CCD) experiment, Design-Expert software, Version 10 (Stat-Ease Inc., USA) was used in this study to plot response surface and analyzed experimental data. The CCD method is a robust and multiparameter optimization statistical technique that employs fewer numbers of experiments to identify and optimize. Volumetric flow rate, packed-bed height, and molar ratio were chosen as independent variables. The molar conversion percentage of palm oil to biodiesel was taken as the response of the designated experiment. Before experimental design, feasibility experiments were performed to determine the ranges of each independent variable. After all, the feasibility experiments provided the basis for this study to provide the optimal range for each factor as well as the desired operating condition for optimum biodiesel conversion in this study. The experimental ranges and levels of independent variables for this study given in Table 1. were chosen based on the feasibility experiments and literature reports. The range of packed-bed height and the volumetric flow rate was set by the column reactor capacity and glass column capabilities. Besides, the reaction temperature was kept constant at room temperature. In most cases, the reaction temperature close to the alcohol boiling point is found to be greatly beneficial and enhances the transesterification process [31]. However, contrary to this study as the high temperature will result in the lower conversion of triglycerides to ethyl esters. It might be due to the unstable hydroxyl group ($-\text{OH}$) of strong base anion exchanger and subjected to degradation when exposed to high temperature even in a short time. Furthermore, the quaternary ammonium groups to transform into tertiary amine groups at elevated temperatures owing to the loss of some nitrogen and thus, its strong basic functionality. Most of the reactions that employed strong base anion exchange are carried out at ambient temperature [15].

As shown in Table 1, the actual levels of the process parameters are 4–12 cm packed bed height, 0.3–0.5 mL min^{-1} volumetric flow rate, and 1:20–1:60 molar ratio palm oil to ethanol. The actual levels and ranges of the process parameters are denoted in coded values as -1 (minimum), 0 (center), $+1$ (maximum), $-\alpha$, $+\alpha$. The distance from the center point of the design space to the star points, also known as alpha (α) was set to 1.682. The factorial design was augmented to CCD to investigate and evaluate the main effects, interaction effects, and quadratic effects of the independent variables on the molar conversion of palm oil to biodiesel. The total number of runs was twenty including 2^3 factorial experiments, 8-star points and 6 replicates to form a central composite design ($2^n + 2n + 6$), where n is the number of factors. The experiments were randomly run to minimize errors between variables and eliminate biases during trials. An empirical model was developed to correlate the response to the transesterification process. It is based on a second-order quadratic model for conversion of palm oil to biodiesel using radiation-induced kenaf as given by Equation (4) to analyze the effect of parameter interactions.

$$C = \beta_0 + \sum_{i=1}^n \beta_i x_i + \sum_{i=1}^n \beta_{ii} x_i^2 + \sum_{i=1}^n \sum_{j=1}^{i-1} \beta_{ij} x_i x_j \quad (4)$$

where C is the response (% molar conversion FAEE); β_0 is the intercept; x_i and x_j are the independent variables or factors; β_i , β_{ii} and β_{ij} are constant coefficients of the linear, quadratic, and interaction effect, respectively.

2.8. Regeneration and Reusability

Regeneration and reusability of the induced VBC-grafted kenaf catalyst in the transesterification of refined palm oil were carried out under the optimum condition in the packed bed reactor. The study was carried out by finding the effect of reusability the same batch of catalyst on the conversion of palm oil. The used catalyst was ready by three regeneration steps as follows: (1) The fiber was taken out from the reactor and washed with HPLC grade ethanol containing 5% (*v/v*) acetic acid to remove the organic substances that covering the active sites of the kenaf catalyst with citrate ion. The removal of fatty acid ion was conducted with the aid of an ultrasonic water bath until the colorless solution and no trace of oil was obtained. The catalyst then was washed with ultrapure water to remove the excess acetic acid solution. (2) The catalyst was regenerated by treated with a 1 M NaOH solution for 1 h. Then, the catalyst was washed with ultrapure water to remove excess NaOH solution. (3) Prior to transesterification in a packed bed reactor, the catalyst was washed with ultrapure water and followed by ethanol to restore the initial swelled condition. The determination of conversion of biodiesel as well as characterization of the fresh and used catalyst was carried out after reusability of the catalyst in each cycle by using HPLC, CHNS elemental analyzer, FE-SEM, and conventional titration method.

3. Result and Discussion

3.1. Catalyst Properties

The surface morphology of fabricated anion exchange kenaf catalyst (VBC-grafted kenaf catalyst) was studied by applying a field emission scanning electron microscope (FESEM) in conjunction with energy-dispersive X-ray spectroscopy (EDX) area analysis. Normally, for quantitative analysis, energy-dispersive X-ray (EDX) is a surface elemental analysis used in conjunction with FESEM and serves the same purpose as a CHNS analysis. Elemental compositions information provided by EDX only on the surface element, meanwhile, CHNS analysis perceives elements throughout the entire substrate. The FESEM micrograph showed significant changes on the surface of raw kenaf fibers after radiation-induced graft polymerization and quaternary amination process (as shown in Supplementary Materials Figure S1). The change of surface texture of kenaf fibers indicates that the fibers' surface was chemically coated result from the introduction of benzylic chlorine groups onto the kenaf cellulosic backbone using VBC. Then, the grafted fiber was further alkylated into quaternary amine functionality using Trimethylamine (TMA). The chemically coated TMA material is observed to flattened on the fiber's surface. It is therefore believed that the TMA is covalently attached to the kenaf surface. Due to the effective radiation-induced graft polymerization and amination, CHNS and EDX analysis detected the abundance of chlorine and ammonia group with the increase in weight percent of Cl and N element (as shown in Supplementary Materials Table S1). TMA group density of the kenaf catalyst measured based on nitrogen content is 2.15 mmol TMA/g-catalyst are comparable to that of commercial granular strong base anion exchange resin (Amberlite® IRA402 resin: 1.93 mmol TMA/g-resin). This attribute to the quaternary ammonia group (NR_4^+) reacted to the grafted VBC-g-kenaf, resulting in a successful synthesis of fiber-based anion exchange catalyst. Besides, the total exchange capacity OH^- of the induced VBC-grafted kenaf catalyst is slightly higher than commercial resin which is 1.3143 and 0.8546 meq g^{-1} , respectively.

The results of surface area, average pore diameter, and total pore volume of studied kenaf fiber show that the graft modification reduces the total area and the pore diameter. The specific surface area for the delignified kenaf calculated by BET analysis was 9.7422 $m^2 g^{-1}$ and characterized as mesopores material, which was reduced to 2.4471 $m^2 g^{-1}$ for the VBC grafted kenaf fiber. Besides, the pore diameter was decreased from 24.3735 to 20.5543 Å, respectively. Thus, grafting on such materials

will shift pore characteristics from mesoporous to microporous. The grafting of the copolymer inside the mesopores causes the total pore volume to decreased from $0.005936 \text{ cm}^3 \text{ g}^{-1}$ before grafting to $0.001257 \text{ cm}^3 \text{ g}^{-1}$ after grafting explained the grafting molecules could easily diffuse into the porous material and react with the inner silanol groups, in that way, decreasing in the pore size and pore volume. This agrees with the observations of previous surface characterization.

3.2. HPLC Analysis

The external calibration curve was constructed for quantification (in mmol) of ethyl oleate, monoolein (MAG), 1,3-diolein (DAG), and triolein (TAG) that presence in palm-oil biodiesel mixture. The regression line of the calibration curve for each standard at the five ranges of concentration was found to be linear with the coefficient of determination (R^2) closer to 1. It can be attributed to the high response of these compounds at the detection wavelength used. Each sample was injected ($5 \mu\text{L}$) in triplicate to obtained precise results from the HPLC analysis.

3.3. Catalyst Screening and Comparison Various Anion Exchanger

The physical and chemical properties and conversion yield of anion exchange kenaf catalyst (NaOH-TMA-VBC-g-kenaf) that has been compared with commercial ion exchange resins (Amberlite[®] IRA402 resin) are summarized in Table 2. The comparison between both anion exchangers was conducted under similar conditions. As shown in Figure 2, the high intensity of FAEs and no presence of triglycerides peaks were recorded in transesterification with anion exchange kenaf catalyst, which indicates high catalytic activity (100% biodiesel conversion). In addition, after completing a 24 h reaction, only one phase final product was observed using the kenaf catalyst. However, Amberlite[®] IRA402 resin has shown a two-phase layer and the lowest yield of FAEs (28.43% conversion) compared to the fabricated anion exchange kenaf catalyst. The presence of triglycerides peaks in the spectra demonstrates that the palm oil was not fully converted using Amberlite[®] IRA402 resin. As expected, this is most likely due to the modified kenaf fiber coated with highly active sites of the trimethylamine group compare to Amberlite[®] IRA402 resin. Furthermore, the speed of reaction using porous anion exchange resins is rather slower than the fibrous type because the catalyst has a reaction site inside the pores and needs a longer time for sample diffusion [12]. Thus, it required a high resin catalyst concentration to accelerate the transesterification process. Surprisingly, anion exchange kenaf is far more astonishing in terms of catalytic performance since it was able to completely convert palm oil to biodiesel with low catalyst concentration (0.1 g) at a low temperature. Since the results of transesterification showed that fabricated anion exchange kenaf catalyst effectively converts oil to biodiesel, thus, it is ready to be loaded in a packed-bed reactor for a continuous transesterification process.

Table 2. Physical and chemical properties of the anion exchanger resin compared to kenaf catalyst.

Catalyst Properties	Details	
Polymeric Material	Plant-based; kenaf	Amberlite [®] IRA402 resin
Functional group	Quaternary ammonium	
Degree of grafting (%)	100	-
Amine group density (mmol g^{-1})	2.1519	1.9348
Total exchange capacity OH^- (meq g^{-1})	1.3143 pa	0.8546
	100%	28%
Biodiesel conversion	At 0.1 g catalyst in 10 g mixture contain 1:50 molar ratio palm oil to ethanol with 24 h reaction time at room temperature (28°C).	

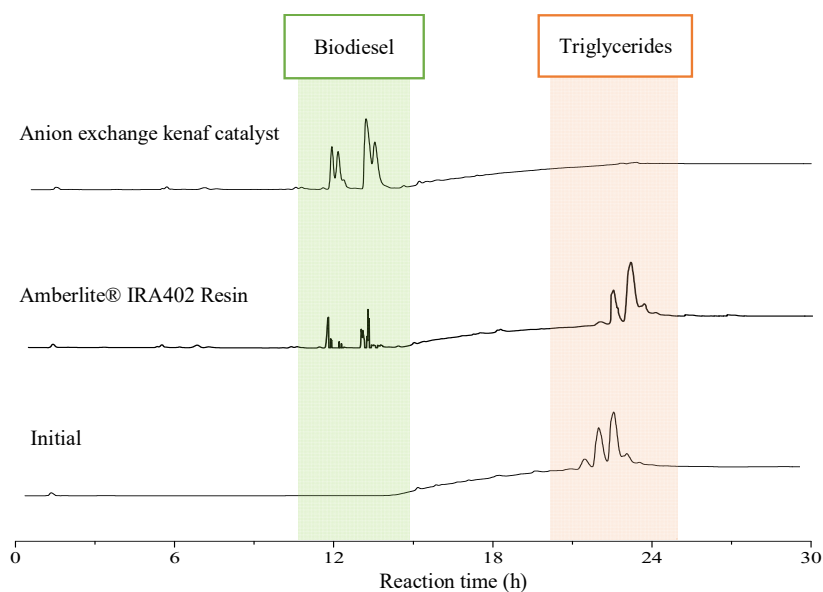


Figure 2. HPLC chromatograms of biodiesel using various types of anion exchangers at the same reaction conditions.

3.4. Response Surface Methodology (RSM)

In the present study, the relationship between response (molar conversion FAEE) and three independent factors (volumetric flow rate, packed-bed height, and molar ratio) was studied. Table 3 provides the performed experiments and results for each experimental run. The independent variables were initially screened by the 2^3 full factorial design with three center points. Based on the result statistical analysis of the screening design data suggesting that the three-dimensional plots of the response are more curvilinear than linear in the design space. Thus, further investigation needs to be done using a higher-order model to determine the optimum conversion for biodiesel within the optimum range of significant variables. The full factorial design data obtained was augmented to a rotatable central composite design (CCD) with an additional three more center points. The total set is 20 experiments in total with eight factorial points, six-star points, and six center points. The second-order polynomial regression equation to predict the conversion of palm oil to biodiesel in terms of coded and actual factors are as below:

$$\text{Molar Conversion (\%)} = -533.17922 + 18.43809A + 575.42907B + 15.81826C + 12.40629AB - 0.087750AC + 0.41983BC - 0.88463A^2 - 950.48521B^2 - 0.13952C^2 \quad (5)$$

From Equation (5), it clearly shows that the quadratic terms indicate the presence of curvatures. It can be referred to as the negative signs in Equation (5) which reveal that the quadratic curves for A^2 , B^2 , and C^2 are concave. Moreover, the positive sign and negative sign in front of the terms suggest synergistic and antagonistic term interaction, respectively. After all, the result statistical analysis of variance (ANOVA) evaluations for response surface quadratic model, shown in Table 4, implies that this model is suitable for the experimental data. This mathematical model was confirmed by a high correlation coefficient and the absence of a lack-of-fit of the model equation to the data. The model F-value is 89.63 which means the model is significant as the value is higher than the theoretical $F_{0.05(5,7)}$ value (3.02) at a 95% confidence level. Besides, the lack of fit was not significant (p -value > 0.05) for the model. The lack of fit value of 2.57 implies that insignificant compare to the pure error. There was a possibility of a 16.16% error occurred due to the noise.

The three variables of packed-bed height (A), volumetric flow rate (B), the molar ratio (C) as well as the interaction of packed-bed height-volumetric flow rate (AB), packed bed height-molar ratio (AC), and quadratic terms of all variables (A^2 , B^2 , C^2) were significant based on the p -value

less than 0.05. The linear term for packed bed height (A) has the largest effect on conversion among the other parameters. In addition, the effect of packed bed height on the molar conversion is most strongly modeled with the quadratic term due to the largest F-value (162.39) and a *p*-value less than 0.0001. Volumetric flow rate (B) and molar ratio (C) have fairly significant effects on the conversion. The interaction of packed-bed height-volumetric flow rate (AB) is the most significant interaction term due to its high F-value (11.08) than the other coupling terms, indicating the positive influence by the combination of the variation in both packed-bed height and volumetric flow rate on biodiesel conversion.

The correlation coefficient value (R^2) estimates the excellence of the model established by the software. As the R^2 value gets closer to 1 (unity), the model is said to be better and gives predicted values closer to the actual. The values of R^2 , adjusted R^2 , and predicted. R^2 for Equation (5) is 0.9878, 0.9767 and 0.9280, respectively. There was an excellent correlation between the experimental data and the predicted data as the R^2 value is 98.78% which was found to be closed to unity. In addition, the closeness value of adjusted R^2 (0.9767) and predicted R^2 (0.9280) is highly acceptable. The adequate precision is the measure of the range in predicted response relative to its associated error and will give a reasonable performance in prediction if the adequate precision value exceeds 4. The ratio for the model is 28.76 which is greater than 4 and the showed an adequate signal. Thus, the model can be employed to navigate the design space.

Table 3. Additional runs to augment the screening design to a central composite design for three variables: axial block with alpha = 1.682.

Standard	Factor 1		Factor 2	Factor 3	Response
	Packed-Bed Height (cm) (Correlation)		Volumetric Flow Rate (mL min ⁻¹)	Ethanol to Oil Ratio	Biodiesel Conversion (%)
Full factorial design					
1	4	(1.40 g)	0.3	40	28.4403
2	12	(4.20 g)	0.3	40	62.0535
3	4	(1.40 g)	0.5	40	3.73408
4	12	(4.20 g)	0.5	40	59.9774
5	4	(1.40 g)	0.3	60	58.1634
6	12	(4.20 g)	0.3	60	80.5165
7	4	(1.40 g)	0.5	60	37.9165
8	12	(4.20 g)	0.5	60	77.3397
9	8	(2.80 g)	0.4	50	89.8107
10	8	(2.80 g)	0.4	50	88.0877
11	8	(2.80 g)	0.4	50	95.9339
Central composite design					
12	1.27	(0.44 g)	0.4	50	20.281
13	14.73	(5.16 g)	0.4	50	87.9478
14	8	(2.80 g)	0.23	50	78.6145
15	8	(2.80 g)	0.57	50	55.9143
16	8	(2.80 g)	0.4	33.18	30.2434
17	8	(2.80 g)	0.4	66.82	79.1290
18	8	(2.80 g)	0.4	50	90.4251
19	8	(2.80 g)	0.4	50	92.6969
20	8	(2.80 g)	0.4	50	90.4251

Table 4. ANOVA for response surface reduced quadratic model: biodiesel conversion.

Source	Sum of Squares	df	Mean Square	F Value	p-Value Prob > F	Remarks
Model	14,342.36	9	1593.60	89.63	<0.0001	Significant
A-Packed bed height	5158.98	1	5158.98	290.17	<0.0001	Significant
B-Volumetric flow rate	571.99	1	571.99	32.17	0.0002	
C-Molar ratio	2424.02	1	2424.02	136.34	<0.0001	
AB	197.01	1	197.01	11.08	0.0076	
AC	98.56	1	98.56	5.54	0.0403	
BC	1.41	1	1.41	0.079	0.7840	Not significant
A ²	2887.13	1	2887.13	162.39	<0.0001	Significant
B ²	1301.95	1	1301.95	73.23	<0.0001	
C ²	2805.25	1	2805.25	157.78	<0.0001	
Residual	177.79	10	17.78			
Lack of Fit	128.00	5	25.60	2.57	0.1616	not significant
Pure Error	49.79	5	9.96			
Cor Total	14,520.15	19				
The R-Squared Results						
R-Squared				0.9878		
Adjusted R-Squared				0.9767		
Predicted R-Squared				0.9280		
Adequate precision				28.755		

3.5. Interaction of Packed-Bed Height and Volumetric Flow Rate

The interaction effect of process variables on a response can be evaluated by studying the three-dimensional surface plot. The plots showing the effect of packed-bed height, volumetric flow rate, molar ratio, and its mutual effect of any two factors by keeping the third variable as a constant. Figure 3a shows there was an increment at the beginning when the volumetric flow rate is increasing along with heightened of packed-bed height. The maximum conversion of palm oil to biodiesel is 95.93% was attained at a volumetric flow rate of around 0.4 mL min⁻¹ and a packed-bed height of 8 cm. However, the decrement in conversion can be seen when the flow rate and packed-bed height beyond the optimum point.

In this experiment work, the mixture (ethanol and palm oil) will only pass through the catalyst at a high flow rate without interacts with the kenaf catalyst, thus failing to exchange the ions between the mixture and kenaf catalyst active sites. At a lower volumetric flow rate of 0.2 mL min⁻¹, poor biodiesel conversion presumably due to insufficient residence time for ample interaction of reactant with catalyst within the column. Moreover, the formation of liquid film on the kenaf catalyst fiber might cause the mass transfer resistance at a low feed flow rate and thus, lowering the conversion. This constraint can be overcome by increase the flow rate that less than the optimum point. Besides, a slight effect on the conversion happened after further increased of packed-bed height higher than 10 cm (>3.50 g). Presumably, this is caused by an overload of a high amount of catalyst which been packed in the column reactor. The excess active sites not accessible to the reaction mixture due to the high catalyst packed.

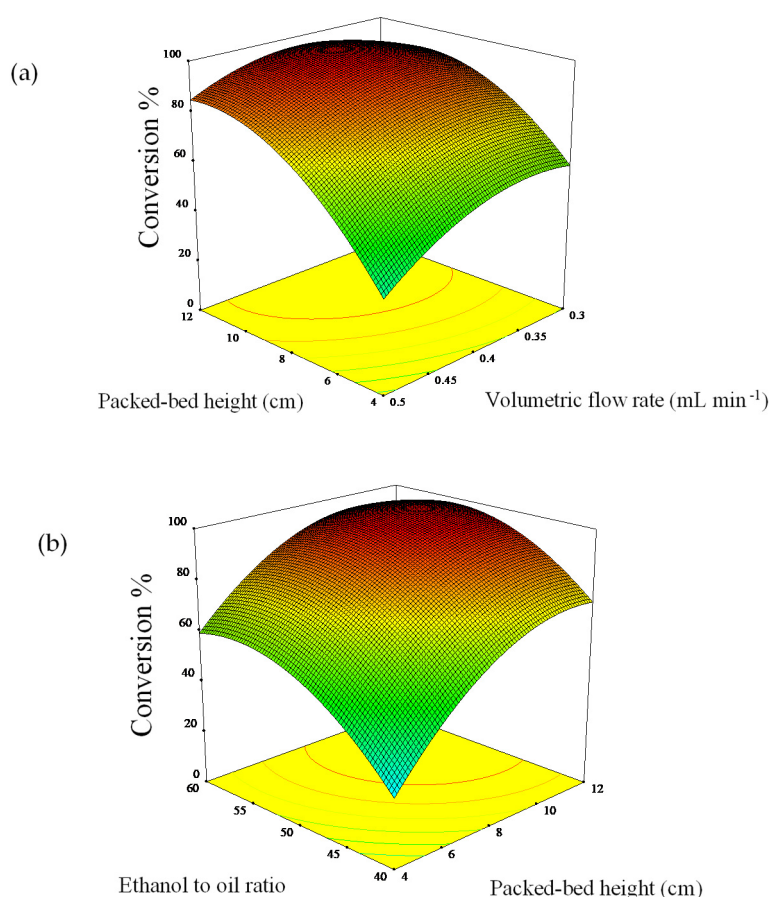


Figure 3. Interaction of (a) packed-bed height and volumetric flow rate and (b) packed-bed height and oil-to-ethanol ratio.

3.6. Interaction of Packed-Bed Height and Oil-to-Ethanol Ratio

The palm oil-to-ethanol ratio has a positive effect on the biodiesel conversion. Higher alcohol than the theoretical ratio (3:1) is required to complete the reaction of transesterification, however, the large excess of alcohol will shift the reaction equilibrium to the left and result in a low yield of biodiesel [1]. The overloading of excess ethanol in the column also might trigger the catalyst saturation and thus, deactivate the catalyst [32]. The three-dimensional surface plot in Figure 3b demonstrates that at 10 cm height of packed kenaf catalyst in the reactor resulted in the maximum conversion of palm oil to biodiesel about 96.01% was gained with an increased ethanol-to-oil molar ratio of 1:50. The decrement of conversion can be seen clearly when at high catalyst loading above 8 cm and a high ethanol-to-oil molar ratio of 50:1.

Our results demonstrated that the optimum molar ratio ethanol to oil is slightly high compared to the universally accepted alcohols to oil molar ratios ranges from 6:1–30:1 [33]. According to [34], transesterification using a heterogeneous catalyst is a complex reaction as it involves three different phases of immiscible liquids of oil, alcohol, and solid catalyst. Initially, considering a three-phase system, the conversion of palm oil into fatty acid ethyl esters is low caused by the mass transfer resistance [35]. For this reason, a high amount of ethanol is needed to compromise between the rate of diffusion and the shifting of the reaction toward biodiesel production. The result of this analysis is then compared with the [9] study, anion AmberlystTM A26 OH resin reported being efficient in the conversion (100%) of soybean oil into biodiesel at optimized conditions of by using extremely high ethanol: soybean oil molar ratio of 150:1 and high amount of anionic resin (50 g), with a reaction time of 24 h, at 78 °C. The noticeable similarity in biodiesel yield can also be seen in the batch-wise catalyst

screening between the fabricated anion exchange kenaf and catalyst Amberlyst™ A26 OH resin might be due to the amount of resin used. Kenaf catalysts required only a small amount to achieve high biodiesel yield at low temperature.

3.7. Optimization

The optimal process conditions for packed-bed height, volumetric flow rate, and molar ratio ethanol to oil were calculated based on the second-order polynomial in Equation (5) generated by ANOVA and correlated with the experimental result. To do this, the desired goal for each of the chosen process factors (A: packed-bed height, B: volumetric flow rate, and C: molar ratio ethanol to oil) defined within the levels range and target value to achieve the maximum conversion of palm oil to biodiesel as stated in Table 5. For the ethanol to palm oil ratio, the target was set to 50:1 to avoid reaction equilibrium shift to the left and catalyst saturation which could reduce the biodiesel yield. Moreover, a large amount of ethanol consumption is less economical for production.

The program identified the maximum overall desirability with respect to the factors based on the response goal. Table 5 shows the optimum conditions giving the maximum calculated conversion palm oil to biodiesel with the total desirability function value of 1. The results of three possible experimental conversions at optimized conditions were found to be close to the generated predicted value with the average percentage error 0.67% which is less than 1% conversion, showing that the regression model was satisfactory. The test number 3 at process conditions of 9.81 cm (3.44 g of packed catalyst in the reactor) packed-bed height, 0.38 mL min⁻¹ volumetric flow rate, and 50:1 ethanol to oil ratio was chosen due to the highest predicted conversion palm oil to biodiesel. The actual result for the biodiesel conversion at optimum condition is 96.87%. In a study conducted by [36], a central composite rotatable design was used to optimize the two process variables which were packed bed height and substrate flow rate for the transesterification of waste cooking palm oil in a packed bed reactor at a reaction of 40 °C which reported an optimum condition for biodiesel yield around 79% at 10.53 cm packed bed height and substrate flow rate of 0.57 mL min⁻¹. The optimum result from [36]'s work is comparable to this present work, however, this present study achieved a greater biodiesel conversion (~95.93%) at a low flow rate (0.38 mL min⁻¹) and (9.81 cm) packed-bed height at room temperature.

In this preliminary study of the use of fabricated fiber-based ion-exchange catalysts for continuous biodiesel production, many important variables were not explored. According to [37], the application for less common catalyst shape in a packed-bed reactor must be subjected to rigorous pilot testing as it is normally known that reactions and mass transfer in a solid-liquid system occur across a catalyst which is yet to be discovered in this study. Therefore, substantial improvement in FAEE conversion is most likely possible through an extensive study on a mathematical model which includes the reaction kinetics and mass transfer for further understanding of fiber-based catalysts behavior and performance in the reactor.

Table 5. The combination of factor levels that maximize the conversion of palm oil to biodiesel.

Factors	Goal	Lower Limit	Upper Limit	Optimal Condition 1	Optimal Condition 2	Optimal Condition 3
Packed-bed height (cm)	In range	4	12	9.43	9.30	9.81
Volumetric flow rate (mL min ⁻¹)	In range	0.3	0.5	0.35	0.37	0.38
Molar ratio	Target			50:1		
Predicted conversion (%)				95.94	96.31	97.29
Actual conversion (%)	Maximize			95.39	95.27	96.87

3.8. Catalyst Reusability

The reusability of the regenerated anion exchange kenaf catalyst was studied to evaluate the stability of the kenaf catalyst in the production of biodiesel at optimum reaction conditions; 9.81 cm packed bed height, a volumetric flow rate of 0.38 mL min⁻¹, and ethanol to palm oil molar ratio at 50:1. The catalytic studies of the fabricated catalyst were carried out by subjected a regeneration

procedure using a selected solvent before proceeding several runs in the packed-bed reactor. Overall, it can be concluded that three main factors cause the poor reusability of kenaf catalyst. First, the fiber dissolution in the washing solvent resulted in weight loss. The second factor is the leaching of the catalyst active sites attached to the kenaf catalyst. Lastly, the surface of the anion exchange kenaf catalyst was impregnated with a range of oils and products.

During the first four reaction cycles of catalyst reusability, the biodiesel yield declined gradually in an increasing number of reuses. The initial catalytic activity of fresh catalyst dropped from 96.9% to 7.2% after fourth-time use. There was no catalytic activity afterward, suggesting low stability and poor reusability. The trend of decreasing in catalyst activity and deterioration in physicochemical properties shown in Figure 4 and Table 6. As shown in Figure 4a, it can be seen that the surface of the fresh catalyst was fully covered with the active site of the amine group, however, with this functional group attached on top of the catalyst surface deteriorated significantly with the increasing number of reuses. The unreacted materials such as glycerol, free fatty acid, excess triglycerides, water, and the brown pigment were said to be adsorbed on the anion-exchanger during the reactive stage of transesterification which then leads to a surface fouling and pore filling of kenaf catalyst. This phenomenon can be observed in Figure 4d where the surface of kenaf appeared oilier and less whitish as before. It is important to highlight the fact that the intricate water-washing process and neutralization steps that are usually performed in batch transesterification using conventional homogeneous catalysts could be avoided due to useful impurities adsorption properties of the catalyst [38]. In results, water containing impurities from this process was greatly reduced, and the biodiesel treatment cost could also be minimized.

The hydroxyl ion ($-OH$) loss from the reused catalyst was confirmed by the drop of total exchange capacity of the regenerated catalyst from 1.3143 to 0.9391 meq g^{-1} after reaction for 8 h in the second run. Followed by 0.7341 and 0.4033 meq g^{-1} in the third run and fourth run, respectively. The weight loss for the kenaf catalyst was observed which is due to the hydrolyzable of kenaf fiber bonds in the amorphous regions during the weak organic acid (acetic acid) washing process. Besides, the use of ethanol as a washing solvent may cause a higher dissolution of fiber in it which then attribute to massive weight loss and degradation. Leaching of the catalyst active sites may also be triggers by ethanol [39–41]. The decrement of nitrogen atom representing the leached active site amine group on the catalyst surface in Table 6 is observed with the increase of reuses number. These reasons that cause a loss in catalyst activity have also been commonly reported by others in the literature [18,28,42,43].

Even though the regeneration ability of anion exchange kenaf fiber significantly drops after first used, it seems that kenaf fiber gave benefits in terms of cost and environmentally friendly material compare to resin type. There is no impending disposal problem of the spent catalyst after use. However, disposal of spent resins must be done in a conditioned form such as by cementation of ion-exchange resins and incinerate the resins, then immobilize the ash which is more complex as it required additional process technology and costs [44].

Table 6. Elemental analysis results for fresh and used anion exchange kenaf catalyst.

Catalyst	Catalytic Activity (%)	Weight Loss (g)	nN (mmol g^{-1})	Total Exchange Capacity (mEq g^{-1})
NaOH-TMA-VBC-g-kenaf (Fresh)	96.9	1.45	2.3430	1.3143
NaOH-TMA-VBC-g-kenaf (2nd cycle)	44.8	1.07	1.8930	1.0391
NaOH-TMA-VBC-g-kenaf (3rd cycle)	12.9	0.43	1.7143	0.7341
NaOH-TMA-VBC-g-kenaf (4th cycle)	7.2	0.26	1.5714	0.4033

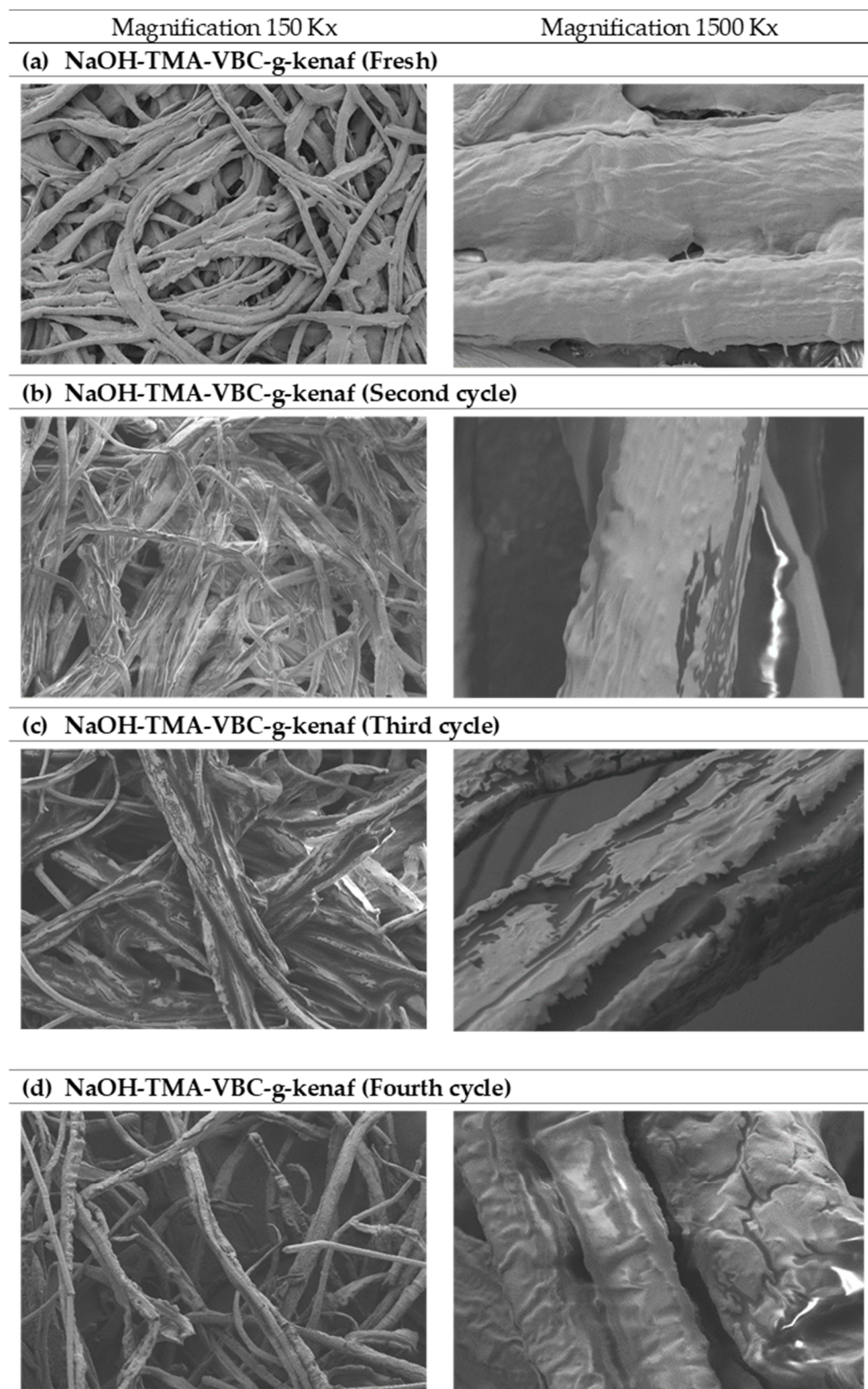


Figure 4. The field emission scanning electron microscope (FESEM) images of (a) NaOH- trimethylamine (TMA)-5 wt%, 4-vinyl-benzylchloride (VBC)-g-kenaf (fresh), (b) NaOH-TMA-VBC-g-kenaf (second cycle), (c) NaOH-TMA-VBC-g-kenaf (third cycle) and (d) NaOH-TMA-VBC-g-kenaf (fourth cycle).

4. Conclusions

In this study, natural fibers can be utilized as catalyst support for grafting copolymerization to produce an anion exchanger catalyst. Catalytic activity for the modified kenaf fiber is more efficient compared to commercial resin since the active sites of kenaf fiber are somewhat more accessible. Moreover, the fabricated anion exchange kenaf catalyst exhibited good performance for the transesterification of refined palm oil with ethanol to produce FAEEs at room temperature in a packed bed reactor. The response surface methodology (RSM) based on the central composite design (CCD) was used to optimize the continuous flow transesterification of palm oil with ethanol in a packed bed reactor. The experimental results showed that RSM is adaptable for the biodiesel conversion studied in this concurrent up-flow transesterification system. The reusability results of the anion exchange kenaf catalyst in the continuous transesterification of refined palm oil under the optimal range conditions show that during the first four reaction cycles of catalyst reusability, the biodiesel yield declined gradually in an increase of reaction time. Though, it is interesting to found out that the anion exchange kenaf catalyst acts as an adsorbent by adsorbed the unreacted materials on the surface of the catalyst. This useful catalyst characteristic can help to reduce cost in biodiesel purification steps. Besides, given the excellent catalytic performances of kenaf-based ion exchange in comparison to resin; it seems that kenaf fiber gave advantages in terms of material cost closer relation to the concept of environmentally material. It has the potential for industrial applications in continuous biodiesel production.

Supplementary Materials: The following are available online at <http://www.mdpi.com/2227-9717/8/10/1289/s1>, Figure S1: FE-SEM images of changes on the surface of kenaf fibers: (a) raw kenaf (b) after radiation-induced graft polymerization, and (c) After quaternary amination process, Table S1: Elemental analysis of delignified kenaf and TMA-VBC-g-kenaf using EDX and CHNS.

Author Contributions: Conceptualization, N.H.Z., L.C.A., N.H.M. and T.S.Y.C.; methodology, N.H.Z., L.C.A., N.H.M. and T.S.Y.C.; investigation, N.H.Z. and N.H.M.; resources, L.C.A. and N.H.M.; visualization, N.H.Z.; supervision, L.C.A., N.H.M. and T.S.Y.C.; project administration, L.C.A. and N.H.M.; funding acquisition, L.C.A. and N.H.M.; writing—original draft preparation, N.H.Z.; writing—review and editing, L.C.A. and N.H.M. All authors have read and agreed to the published version of the manuscript.

Funding: This research was funded by the Ministry of Higher Education Funding FRGS Grant (FRGS/1/2019/TK05/UPM/01/1) and ScienceFund Grant (03-03-01-SF0253) from the Ministry of Science, Technology, and Innovation of Malaysia (MOSTI).

Acknowledgments: The authors acknowledge sincerely the Electron Beam Irradiation Facility (ALURTRON), Radiation Processing Division Malaysian Nuclear for supporting and encouraging this investigation.

Conflicts of Interest: The authors declare no conflict of interest.

References

1. Demirbas, A. Progress and recent trends in biodiesel fuels. *Energy Convers. Manag.* **2009**, *50*, 14–34. [[CrossRef](#)]
2. Atabani, A.; Silitonga, A.; Badruddin, I.A.; Mahlia, T.; Masjuki, H.; Mekhilef, S. A comprehensive review on biodiesel as an alternative energy resource and its characteristics. *Renew. Sustain. Energy Rev.* **2012**, *16*, 2070–2093.
3. Masjuki, H.H.; Abul, K.M. An overview of biofuel as a renewable energy source: Development and challenges. *Procedia Eng.* **2013**, *56*, 39–53.
4. Mahmud, M.I.; Cho, H.M. A review on characteristics, advantages and limitations of palm oil biofuel. *Int. J. Glob. Warm.* **2018**, *14*, 81–96. [[CrossRef](#)]
5. Noor, C.W.M.; Noor, M.M.; Mamata, R. Biodiesel as alternative fuel for marine diesel engine applications: A review. *Renew. Sustain. Energy Rev.* **2018**, *94*, 127–142. [[CrossRef](#)]
6. Faba, E.M.S.; Ferrero, G.O.; Dias, J.M.; Eimer, G.A. Alternative raw materials to produce biodiesel through alkaline heterogeneous catalysis. *Catalysts* **2019**, *9*, 1–14.
7. Guo, F.; Fang, Z. Biodiesel production with solid catalysts. In *Biodiesel—Feedstocks and Processing Technologies*; Stoytcheva, M., Ed.; Intech Open: London, UK, 2011.

8. Tacias-Pascacio, V.G.; Torrestiana-Sanchez, B.; Magro, L.D.; Virgen-Ortiz, J.J.; Suárez-Ruíz, F.J.; Rodrigues, R.C.; Fernandez-Lafuente, R. Comparison of acid, basic and enzymatic catalysis on the production of biodiesel after RSM optimization. *Renew. Energy* **2019**, *135*, 1–9. [[CrossRef](#)]
9. Oliveira, E.V.A.; Costa, L.C.; Thomaz, D.M.; Costa, M.A.S.; Maria, L.C.S. Transesterification of soybean oil to biodiesel by anionic and cationic ion exchange resins. *Rev. Virtual Química* **2015**, *7*, 2314–2333. [[CrossRef](#)]
10. Semwal, S.; Arora, A.K.; Badoni, R.P.; Tuli, D.K. Biodiesel production using heterogeneous catalysts. *Bioresour. Technol.* **2011**, *102*, 2151–2161. [[CrossRef](#)]
11. Shibasaki-Kitakawa, N.; Tsuji, T.; Kubo, M.; Yonemoto, T. Biodiesel production from waste cooking oil using anion-exchange resin as both catalyst and adsorbent. *Bioener. Res.* **2011**, *4*, 287–293. [[CrossRef](#)]
12. Ueki, Y.; Mohamed, N.H.; Seko, N.; Tamada, M. Rapid biodiesel fuel production using novel fibrous catalyst synthesized by radiation-induced graft polymerization. *Int. J. Org. Chem.* **2011**, *1*, 20–25. [[CrossRef](#)]
13. Inamuddin, D.; Luqman, M. *Ion Exchange Technology I: Theory and Materials*; Springer: London, UK, 2012.
14. Abdullah, S.H.Y.S.; Hanapi, N.H.M.; Azid, A.; Umar, R.; Juahir, H.; Khattoon, H.; Endut, A. A review of biomass-derived heterogeneous catalyst for a sustainable biodiesel production. *Renew. Sustain. Energy Rev.* **2017**, *70*, 1040–1051. [[CrossRef](#)]
15. Jamil, F.; Al-Haj, L.; Al-Muhtaseb, A.H.; Al-Hinai, M.A.; Baawain, M.; Rashid, U.; Ahmad, M.N. Current scenario of catalysts for biodiesel production: A critical review. *Rev. Chem. Eng.* **2018**, *34*, 267–297. [[CrossRef](#)]
16. Zabarruddin, N.H.; Mohamed, N.H.; Abdullah, L.C.; Tamada, M.; Ueki, Y.; Seko, N.; Choong, T.S.Y. Palm oil-based biodiesel synthesis by radiation-induced kenaf catalyst packed in a continuous flow system. *Ind. Crop. Prod.* **2019**, *136*, 102–109. [[CrossRef](#)]
17. Chakraborty, R.; Bepari, S.; Banerjee, A. Application of calcined waste fish (*Labeo rohita*) scale as low-cost heterogeneous catalyst for biodiesel synthesis. *Bioresour. Technol.* **2011**, *102*, 3610–3618. [[CrossRef](#)]
18. Borges, M.E.; Díaz, L. catalytic packed-bed reactor configuration for biodiesel production using waste oil as feedstock. *BioEnergy Res.* **2012**, *6*, 222–228. [[CrossRef](#)]
19. Tan, Y.H.; Abdullah, M.O.; Kandedo, J.; Mubarak, N.M.; Chan, Y.S.; Nolasco-Hipolito, C. Biodiesel production from used cooking oil using green solid catalyst derived from calcined fusion waste chicken and fish bones. *Renew. Energy* **2019**, *139*, 696–706. [[CrossRef](#)]
20. Ogunkunle, O.; Oniya, O.O.; Adebayo, A.O. Yield response of biodiesel production from heterogeneous and homogeneous catalysis of milk bush seed (*Thevetia Peruviana*) oil. *Energy Policy Res.* **2017**, *4*, 21–28. [[CrossRef](#)]
21. Baskar, G.; Selvakumari, I.A.E.; Aiswarya, R. Biodiesel production from castor oil using heterogeneous Ni doped ZnO nanocatalyst. *Bioresour. Technol.* **2018**, *250*, 793–798. [[CrossRef](#)]
22. Orlando, U.S.; Baes, A.U.; Nishijima, W.; Okada, M. A new procedure to produce lignocellulosic anion exchangers from agricultural waste materials. *Bioresour. Technol.* **2002**, *83*, 195–198. [[CrossRef](#)]
23. Moawia, R.M.; Nasef, M.M.; Mohamed, N.H. Radiation grafted natural fibres functionalized with alkalised amine for transesterification of cottonseed oil to biodiesel. *J. Teknol.* **2016**, *78*, 89–93. [[CrossRef](#)]
24. Liu, X.; Linb, R.; Chen, S.; Ma, N.; Huang, Y. Preparation of a bagasse-based anion exchange fiber for sugar decolorization. *J. Appl. Polym. Sci.* **2012**. [[CrossRef](#)]
25. Rudie, A.W.; Ball, A.; Patel, N. Ion Exchange of H⁺, Na⁺, Mg²⁺, Ca²⁺, Mn²⁺, and Ba²⁺, on Wood Pulp. *J. Wood Chem. Technol.* **2006**, *26*, 259–272. [[CrossRef](#)]
26. Tabatabaei, M.; Aghbashlo, M. *Biodiesel from Production to Combustion*; Gupta, V.K., Tuohy, M.G., Eds.; Springer Nature: Cham, Switzerland, 2019; Volume 8.
27. Stamenković, O.S.; Veličković, A.V.; Veljković, V. The production of biodiesel from vegetable oils by ethanolysis: Current state and perspectives. *Fuel* **2011**, *90*, 3141–3155. [[CrossRef](#)]
28. Shibasaki-Kitakawa, N.; Honda, H.; Kuribayashi, H.; Toda, T.; Fukumura, T.; Yonemoto, T. Biodiesel production using anionic ion-exchange resin as heterogeneous catalyst. *Bioresour. Technol.* **2007**, *98*, 416–421. [[CrossRef](#)] [[PubMed](#)]
29. Zhao, X.; Wei, L.; Cheng, S.; Julson, J. Review of heterogeneous catalysts for catalytically upgrading vegetable oils into hydrocarbon biofuels. *Catal.* **2017**, *7*, 83. [[CrossRef](#)]
30. Mohamed, N.H.; Tamada, M.; Ueki, Y.; Seko, N. Effect of partial delignification of kenaf bast fibers for radiation graft copolymerization. *J. Appl. Polym. Sci.* **2012**, *127*, 2891–2895. [[CrossRef](#)]
31. Zabeti, M.; Daud, W.M.A.W.; Aroua, M. Activity of solid catalysts for biodiesel production: A review. *Fuel Process. Technol.* **2009**, *90*, 770–777. [[CrossRef](#)]

32. Lau, P.C.; Kwong, T.-L.; Yung, K.-F. Effective heterogeneous transition metal glycerolates catalysts for one-step biodiesel production from low grade non-refined Jatropha oil and crude aqueous bioethanol. *Sci. Rep.* **2016**, *6*, 23822. [[CrossRef](#)]
33. Balat, M.; Balat, H. A critical review of bio-diesel as a vehicular fuel. *Energy Convers. Manag.* **2008**, *49*, 2727–2741. [[CrossRef](#)]
34. Fattah, I.M.R.; Ong, H.C.; Mahlia, T.M.I.; Mofijur, M.; Silitonga, A.S.; Rahman, S.M.A.; Ahmad, A. State of the art of catalysts for biodiesel production. *Front. Energy Res.* **2020**, *8*. [[CrossRef](#)]
35. Musa, I.A. The effects of alcohol to oil molar ratios and the type of alcohol on biodiesel production using transesterification process. *Egypt. J. Pet.* **2016**, *25*, 21–31. [[CrossRef](#)]
36. Halim, S.F.A.; Kamaruddin, A.H.; Fernando, W. Continuous biosynthesis of biodiesel from waste cooking palm oil in a packed bed reactor: Optimization using response surface methodology (RSM) and mass transfer studies. *Bioresour. Technol.* **2009**, *100*, 710–716. [[CrossRef](#)] [[PubMed](#)]
37. Afandizadeh, S.; Foumeny, E. Design of packed bed reactors: Guides to catalyst shape, size, and loading selection. *Appl. Eng.* **2001**, *21*, 669–682. [[CrossRef](#)]
38. Bazooyar, B.; Ghorbani, A.; Shariati, A. Physical properties of methyl esters made from alkali-based transesterification and conventional diesel fuel. *Energy Sour. Part A: Recover. Util. Environ. Eff.* **2015**, *37*, 468–476. [[CrossRef](#)]
39. Pekhtasheva, E.; Neverov, A.; Kubica, S.; Zaikov, G. Biodegradation and biodeterioration of some natural polymers. *Chem. Chem. Technol.* **2012**, *6*, 263–280. [[CrossRef](#)]
40. Trygg, J.; Trivedi, P.; Fardim, P. Controlled depolymerisation of cellulose to a given degree of polymerisation. *Cell. Chem. Technol.* **2016**, *50*, 557–567.
41. Trygg, J.; Fardim, P. Enhancement of cellulose dissolution in water-based solvent via ethanol–hydrochloric acid pretreatment. *Cellulose* **2011**, *18*, 987–994. [[CrossRef](#)]
42. Baroutian, S.; Aroua, M.; Raman, A.A.A.; Sulaiman, N.M. A packed bed membrane reactor for production of biodiesel using activated carbon supported catalyst. *Bioresour. Technol.* **2011**, *102*, 1095–1102. [[CrossRef](#)]
43. Ren, Y.; He, B.; Yan, F.; Wang, H.; Cheng, Y.; Lin, L.; Feng, Y.; Li, J. Continuous biodiesel production in a fixed bed reactor packed with anion-exchange resin as heterogeneous catalyst. *Bioresour. Technol.* **2012**, *113*, 19–22. [[CrossRef](#)]
44. IAEA (Ed.) *Treatment of Spent Ion-Exchange Resins for Storage and Disposal*; Technical Reports Series No. 254; IAEA: Vienna, Austria, 1985.



© 2020 by the authors. Licensee MDPI, Basel, Switzerland. This article is an open access article distributed under the terms and conditions of the Creative Commons Attribution (CC BY) license (<http://creativecommons.org/licenses/by/4.0/>).